GeoScienceWorld
Lithosphere
Volume 2022, Article ID 2039170, 13 pages
https://doi.org/10.2113/2022/2039170

Lithosphere

Research Article

Distribution of ^{222}Rn in Seawater Intrusion Area and Its Implications on Tracing Submarine Groundwater Discharge on the Upper Gulf of Thailand

Yancheng Wang,[1,2] **Guangquan Chen**,[1,2] **Hongjun Yu**,[1,2] **Xingyong Xu**,[3] **Wenquan Liu**,[1,2] **Tengfei Fu**,[1,2] **Qiao Su**,[1,2] **Yinqiao Zou**,[1,2] **Narumol Kornkanitnan**,[4] **and Xuefa Shi**[1,2]

[1]*Key Laboratory of Marine Geology and Metallogeny, First Institute of Oceanography, Ministry of Natural Resources, Qingdao 266061, China*
[2]*Laboratory for Marine Geology, Qingdao National Laboratory for Marine Science and Technology, Qingdao 266237, China*
[3]*Fourth Institute of Oceanography, Ministry of Natural Resources, Beihai 266061, China*
[4]*Marine and Coastal Resources Research and Development Institute, Department of Marine and Coastal Resources, Bangkok 10210, Thailand*

Correspondence should be addressed to Guangquan Chen; chenguangquan@fio.org.cn

Received 9 March 2022; Accepted 7 June 2022; Published 16 June 2022

Academic Editor: Hema Achyuth

Radon (^{222}Rn) has been widely employed as a tracer for estimating submarine groundwater discharge (SGD). However, the uncertainty of the SGD estimation remains significant, due to the spatial variability of radon in groundwater. In this study, we analyzed the hydrochemical proprieties of seawater and coastal groundwater in the Upper Gulf of Thailand and discussed the distribution characteristics of ^{222}Rn in aquifers in terms of aquifer lithology, groundwater system recharge conditions, and water retention time. The results suggested that the residence time of groundwater and the process of groundwater salinization have the greatest impact on the distribution of ^{222}Rn activity. A ^{222}Rn mass balance model, synthesizing the distribution characteristics of ^{222}Rn in groundwater and tidal influences on SGD, was built to estimate the submarine groundwater discharge in the Upper Gulf of Thailand. The result showed that the SGD flux of the Upper Gulf of Thailand was 0.0203 m/d. Moreover, there is a positive correlation between tidal height and the activity of ^{222}Rn in groundwater. The SGD observed during the low tide was about 1.25 times higher than that observed during the high tide. This may influence the marine geochemical cycles of elements and their impact on marine ecosystems.

1. Introduction

Submarine groundwater discharge (SGD), which includes both fresh and saline groundwater outflows to seas, has been considered an important contributor to the water and chemical budgets of the world's oceans [1, 2]. It is an important process for the marine biogeochemical cycles of elements, such as nutrients, trace metals, carbon, and rare earth elements [3–7]. SGD is recognized as an "invisible" process, driven by both marine and terrestrial forcing components below the water surface. Different types of groundwater can be mixed with the water through the coastal subsurface sediments to form subterranean estuaries, transporting nutrients in coastal ecosystems, which can affect water quality and lead to environmental deterioration in coastal areas [8]. Hence, understanding SGD is important for the management of coastal waters.

The natural radioisotopes radium (Ra) and radon (Rn) have a wide range of applications in investigating SGD fluxes [4, 9–12]. Indeed, natural radioisotopes show the advantage of a composite tracer signal when entering the ocean by a variety of routes in the aquifer due to their conservative behavior [13]. ^{222}Rn, with a half-life of 3.8 days, was considered to be an excellent tracer for quantifying submarine groundwater discharge [10, 13]. The ^{222}Rn mass balance

model proposed by Burnett and Charette et al. was used to evaluate the SGD. The model assumed that the water body was well mixed and there was no water stratification in terms of ^{222}Rn distribution. The estimation of mixing loss was a speculative value, which would lead to some errors in the results. Methods for estimating SGD using chemical tracers are also being improved; for example, Lamontagne and Webster described how to better estimate SGD from trends in the chemical fingerprint in seawater [14, 15]. Although quantifying SGD remains challenging because of its spatial and temporal variability, a classical mass balance model for SGD estimation has been applied or accepted by many researchers to estimate SGD [8, 16–19]. The ^{222}Rn mass balance model of estimating SGD flux is based on converting ^{222}Rn inventories to the flux of Rn derived from the SGD by considering both the Rn distributions in sea water and groundwater inflowing to the coastal zone and taking into account radioactive decay, tidal effects, river input, sediment diffusion, atmospheric escape, and mixing with low-concentration offshore waters [13]. In order to transform ^{222}Rn fluxes to SGD fluxes, the radon end-member in the groundwater needs to be determined. Due to the high spatial variability of the radon isotope in groundwater, large uncertainty in the model calculation can be observed. However, most studies of SGD have been primarily focusing on estimating the fluxes of Rn without assessing the distribution of ^{222}Rn in the groundwater end-member [20].

The coastline of Thailand's coastal regions has changed due to natural and human influences, resulting in environmental degradation and hydraulic balance change [21]. Indeed, groundwater and coastal water pollution is the main problem encountered in Thailand's coastal regions [22, 23]. However, groundwater discharge may be easily overlooked as a hidden channel, even though it carries significant amount of nutrients and pollutants.

In addition to reducing groundwater pollution, it is also important to effectively identify the exchange process between groundwater and seawater. As an inert gas, the geochemical behavior of Rn is relatively conservative in aquifers and becomes significantly enriched in SGD fluids compared to seawater [10]. Therefore, ^{222}Rn is widely used to estimate SGD fluxes, allowing the identification of groundwater discharge hotspots and pollution sources, thus facilitating targeted treatment in the study area [23, 24].

Due to the low-lying area proximity to the sea and the deep well pumping [25], the sea-level rise, land subsidence, and seawater intrusion have occurred in the Gulf of Thailand [26]. Salinization in freshwater aquifers can cause water–rock interaction, increasing total dissolved solid (TDS) concentrations and the risk of contamination of water resources [27]. Indeed, the salinity of groundwater has long been considered to be the primary factor affecting the Ra activity in the SGD end-member. Cerdà-Domènech et al. [20] showed that the desorption of Ra increases significantly with the increase of salinity. The spatial variability in the distribution of ^{226}Ra may lead to changes in the ^{222}Rn concentrations. Indeed, the groundwater salinization process leads to spatial heterogeneity of radioisotope activity in aquifers [27], thus causing great uncertainty in the SGD assessment.

In this study, the hydrochemical characteristics of groundwater along the Upper Gulf of Thailand were assessed to reveal the impact of sea intrusion groundwater quality. In addition, comprehensive monitoring was carried out to assess the spatiotemporal distribution of ^{222}Rn in seawater and coastal groundwater and to calculate the SGD accurately in the upper Gulf of Thailand. Moreover, the present study is aimed at estimating the SGD fluxes in the East coast and the entire Upper Gulf of Thailand based on the characteristics of ^{222}Rn distribution results and at analyzing the spatiotemporal changes in groundwater in coastal areas under the influence of tides. The research results are of great significance for the protection of ecological environment and groundwater resources in coastal areas of Thailand.

2. Materials and Methods

2.1. Study Area. This study was conducted in the Upper Gulf of Thailand and its coastal sections (Figure 1). The Gulf of Thailand covers an area of about 320,000 km^2 [21]. Malaysia, Thailand, Cambodia, and Vietnam share this semienclosed tropical sea in the South China Sea (Pacific Ocean). The terrain in Thailand is high in the north and low in the south. On the other hand, river networks are densely dispersed from North to South and run into the Gulf of Thailand. The Upper Gulf is U-shaped and forms the catchment basin of two rivers in the western coast and four major rivers in its Northern part (Bang Pakong, Chao Phraya, Tha Chin, and Mae Klong Rivers) [28].

The study area belongs to a part of the Chao Phraya Plain which is a fault-bounded basin developed in the Polio-Pleistocene epoch. The main aquifers in this area consist of fluvial deposits and marine sediments, and aquitard layers of clay separate the aquifers from one another [26]. There are eight different aquifers in the Chao Phraya-Tha Chin Basin less than 700 m deep from surface level (Figure 2). They are confined aquifers and are on average 50 m thick. These aquifers and the depth from ground surface level (m) can be summarized as follows [29]: (1) Bangkok 50; (2) Phra Pradeang 100; (3) Nakhon Luang 150; (4) Nonthaburi 200; (5) Sam Khok 300; (6) Phaya Thai 350; (7) Thon Buri 450; and (8) Pak Nam 550.

The Gulf of Thailand is a vital source of the Thai economy. Indeed, the fishing sector, tourism, and port activities in the Gulf region have brought great benefits to the residents. In recent decades, with increasing population, as well as industrial and economic development, several coastal development projects have been planned and implemented. However, these projects have impacted local coastal and estuarine formations, resulting in changes in coastal processes and shorelines. Furthermore, the offshore area has become severely polluted [21, 23]. The causes of coastal groundwater and seawater pollution in Thailand are surface runoff and drainage of effluents from port, urban, and industrial areas. Moreover, rivers and groundwater are highly polluted by urban sewage, industrial wastewater, and sediments.

The upper Gulf's surface water quality is often poor, particularly around the downstream of the four major rivers

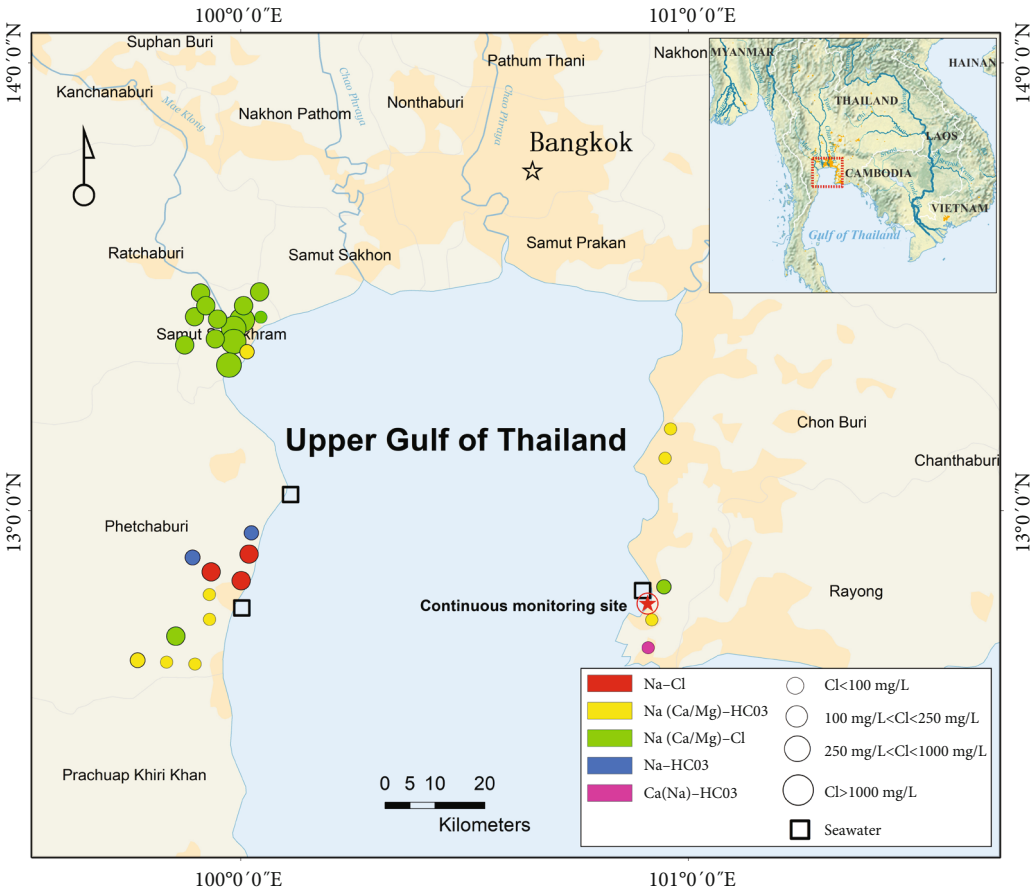

Figure 1: Chemical compositions of water samples from the Upper Gulf of Thailand.

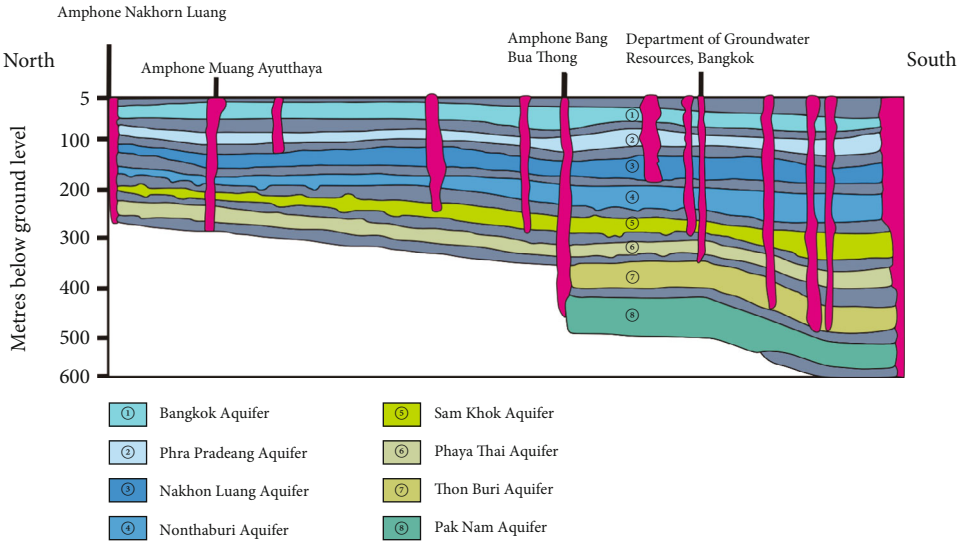

Figure 2: Aquifers in Chao Phraya River Basin (modified by Fornés and Pirarai [29]).

and important tourist destinations along the coast [21]. Water quality in the upper Gulf region is deteriorating due to the increased use of nitrogen fertilizers, mariculture activity, and urban waste.

2.2. Water Sampling. In total, 32 water samples of the Gulf of Thailand's coastline were collected from May to November 2018 for hydrochemical analysis (Table 1). The samples consisted of 29 groundwater and 3 seawater samples collected

Table 1: Geographical coordinates of the sampling points.

Sample code	Latitude N	Longitude E	Depth (m)	Sample code	Latitude N	Longitude E	Depth (m)
TW1	12.663	99.802	70	TW17	13.431	100.003	36
TW2	12.659	99.826	26	TW18	13.442	100.018	105
TW3	12.657	99.850	32	TW19	13.395	99.925	89
TW4	12.722	99.851	71	TW20	13.414	99.946	80
TW5	12.773	99.907	33	TW21	13.420	99.951	100
TW6	12.783	99.913	54	TW22	13.422	99.956	97
TW7	12.878	99.905	16	TW23	13.425	99.946	112
TW8	12.868	99.919	27	TW24	13.452	99.943	120
TW9	12.815	99.990	85	TE1	12.704	100.892	5
TW10	12.882	100.009	90	TE2	12.764	100.896	8
TW11	12.925	100.024	140	TE3	12.821	100.913	3
TW12	13.377	99.995	100	TE4	13.129	100.972	15
TW13	13.376	99.989	60	TE5	13.164	100.971	14
TW14	13.408	99.971	15	TWS1	12.793	99.984	
TW15	13.420	99.996	60	TWS2	13.041	100.093	
TW16	13.417	100.031	126	TES1	12.821	100.914	

TWS1, TWS2, and TES1 are seawater samples, while the remaining are groundwater samples.

from residential wells and estuarine seawater, respectively (Figure 1).

2.3. Continuous Monitoring of ^{222}Rn. The RAD-7 continuous monitoring system with a submersible pump was installed in the offshore groundwater of the eastern coastal zone (100.90° E, 12.77° N) to continuously monitor (24 hours) ^{222}Rn. The monitoring was carried out every 2 hours, from 15:15 on November 23 to 17:15 on November 24, 2018 (Figure 1). In addition, tidal data were collected to compare the effect of tidal height on SGD.

2.4. Analytical Methods. Total dissolved solids (TDS) and pH were measured using a portable multiparameter water quality analyzer (YSI Pro Plus, American YSI). To purify the samples and prevent air from entering, the water sample was first filtered via a 0.45 μm membrane filter and then placed in a bubble-free polyethylene bottle and sealed with an adhesive stripe. Finally, all samples were stored strictly in cold storage before being sent to the laboratory.

The K^+, Na^+, Ca^{2+}, Mg^{2+}, Br^-, and ^{238}U were analyzed using an inductively coupled plasma-atomic emission spectrometer (ICP-MS, American Thermo Fisher). Cl^- and SO_4^{2-} were determined by an ion chromatograph (ICS-3000, American DIONEX). A titration method with phenolphthalein solution and standard HCl solution was used to analyze the HCO_3^- [30, 31].

To assess the activity of ^{222}Rn, the water samples were slowly injected into a 250 mL glass bottle, in which ^{222}Rn was analyzed using a RAD-7 radon monitor and its RAD H_2O water accessory. The ^{222}Rn activity was determined continuously in coastal groundwater using radon automatic monitoring systems [32]. The radon automatic monitoring systems worked by providing a constant stream of water (driven by a submersible pump) to be analyzed to the RAD-7. Continuous activity of ^{222}Rn in groundwater can be obtained by setting the pumping time [10].

3. Results and Discussion

3.1. Hydrochemistry

3.1.1. Major Ion Contents. The hydrochemical results (Table 2) showed that Cl^- was the dominating anion in most groundwater samples, followed by HCO_3^-, while Na^+ was the dominating cation, followed by Ca^{2+} and Mg^{2+}. In addition, the ranges of TDS, Cl^-, HCO_3^-, Na^+, Ca^{2+}, and Mg^{2+} concentrations in groundwater samples were 96.43-5092.52, 17.88-3788.00, 69.78-652.10, 17.70-533.10, 14.69-299.10, and 2.71-157.40 mg/L, respectively.

Based on the location and chemical compositions of groundwater samples (Figure 1), the study area was divided into three main areas, namely, the southwestern area (TW1-TW11), the northwestern area (TW12-TW24), and the eastern area (TE1-TE5). The hydrochemical type of groundwater on the southwestern area is mainly Na-HCO_3 and Na-Cl. The hydrochemical type of groundwater on the northwestern area is Na-Cl. The hydrochemical type of groundwater on the eastern area is mainly Na-HCO_3 and Ca-HCO_3.

The pH of groundwater in the southwestern area ranged from 6.76 to 7.98, with an average value of 7.36. The range of TDS was 386.01-1417.01 mg/L, with an average of 792.93 mg/L. The results showed that Na^+ was the dominant cation in the groundwater of the southwestern area, ranging from 87.94 to 442.40 mg/L, with an average of 190.19 mg/L, while the dominant anion was HCO_3^-, ranging from 341.27 to 652.10 mg/L, with an average value of 465.43 mg/L.

Table 2: Element concentrations and activity of ^{222}Rn in groundwater and seawater in the Gulf of Thailand.

Sample code	pH	TDS (mg/L)	K^+ (mg/L)	Na^+ (mg/L)	Ca^{2+} (mg/L)	Mg^{2+} (mg/L)	Cl^- (mg/L)	SO_4^{2-} (mg/L)	HCO_3^- (mg/L)	Br^- (mg/L)	^{238}U (μg/L)	^{222}Rn (Bq/m^3)
TW1	6.97	666.44	14.67	103.30	40.14	45.96	137.60	10.78	627.99	7.26	7.47	47119.07
TW2	7.10	600.59	10.64	112.70	29.24	46.97	67.60	7.39	652.10	1.85	2.77	49858.91
TW3	7.64	445.54	14.28	114.90	17.57	31.50	30.99	4.13	464.33	0.00	19.19	3863.10
TW4	7.37	877.60	21.02	137.30	95.33	51.95	382.60	11.79	355.23	2.69	57.30	15758.93
TW5	6.97	386.01	11.25	87.94	45.29	9.23	58.60	3.07	341.27	2.66	35.10	34350.45
TW6	7.44	482.21	11.95	101.80	68.02	13.39	54.80	8.65	447.21	0.10	108.00	27494.86
TW7	7.20	706.83	6.44	163.80	58.07	29.32	161.60	79.86	415.49	1.10	59.41	11733.63
TW8	6.76	1323.41	10.01	294.90	103.20	49.88	540.50	94.02	461.79	15.59	72.89	21996.34
TW9	7.67	1417.01	12.19	442.40	50.13	33.35	626.00	35.69	434.52	4.21	41.91	6296.81
TW10	7.81	914.22	8.45	288.30	26.21	19.35	280.00	53.40	477.02	0.97	26.77	3247.75
TW11	7.98	902.35	8.37	244.80	26.83	25.33	224.60	151.04	442.76	0.40	41.78	2874.06
TW12	7.40	5092.52	17.85	533.10	299.10	157.40	3788.00	146.10	301.94	3.77	31.21	14121.42
TW13	7.36	2142.21	15.55	362.50	187.70	121.30	1200.60	111.20	286.72	3.09	23.74	12319.31
TW14	7.33	2888.57	17.86	468.70	257.50	132.20	1697.00	171.00	288.62	5.39	24.67	18222.63
TW15	6.67	2345.57	2.78	100.30	64.55	42.01	1938.00	42.52	310.82	4.91	4.04	9007.98
TW16	7.74	683.54	7.25	156.90	38.89	41.77	213.00	44.95	361.57	0.96	3.27	21178.95
TW17	7.18	1691.87	9.16	236.00	179.20	112.10	951.50	31.06	345.71	2.55	23.69	7686.57
TW18	6.82	1252.78	7.83	220.30	97.46	70.43	649.00	23.80	367.91	7.50	13.88	9242.51
TW19	6.98	1794.42	19.37	330.20	230.90	69.25	788.20	249.30	214.40	2.47	5.23	7488.49
TW20	7.02	1109.95	10.96	220.20	109.20	66.92	373.40	129.45	399.63	1.35	25.47	17584.54
TW21	7.08	1009.45	9.99	197.10	93.51	59.25	362.60	80.52	412.95	0.98	16.11	4563.08
TW22	7.06	1174.60	10.53	210.30	106.00	66.74	508.50	76.20	392.65	1.71	17.15	10114.11
TW23	7.45	1085.64	10.05	186.90	104.80	69.13	472.40	53.65	377.43	1.48	15.30	3576.08
TW24	7.41	1819.84	15.53	282.20	177.50	91.01	932.20	170.75	301.31	1.92	23.74	1720.74
TE1	6.74	380.96	11.84	54.08	55.13	14.08	51.94	61.31	265.15	0.90	1.68	38215.42
TE2	6.39	346.82	14.21	65.90	55.63	9.65	62.04	68.98	140.82	0.90	1.41	4194.34
TE3	6.94	626.78	6.92	143.40	64.01	6.77	190.90	143.41	142.73	0.00	1.30	987.96
TE4	6.34	312.22	11.60	50.39	44.42	9.67	42.68	76.08	154.78	0.20	2.00	9908.01
TE5	5.11	96.43	3.18	17.70	14.69	2.71	17.88	5.39	69.78	0.20	1.70	36515.76
TWS1	8.07	13677.83	10.90	215.30	7.60	23.44	11840.00	1507.00	147.17	41.06	0.34	108.13
TWS2	7.95	11650.98	11.36	219.20	7.77	23.82	10044.00	1276.00	137.65	39.23	0.32	42.28
TES1	8.18	15974.33	531.90	3104.00	273.00	444.70	9170.00	2380.00	141.46	33.54	4.25	108.86

Regarding the anions, the contents of HCO_3^- and Cl^- raised alternately, while the contents of SO_4^{2-} were very low in Figure 3. The hydrochemical types of groundwater were mainly Na-HCO_3 and Na-Cl, suggesting a slight intrusion of seawater in this area, which leads to the increase in Cl^- and Na^+.

The pH of groundwater in the northwestern area varied from 6.67 to 7.74, with an average of 7.19. The variation range of TDS was relatively large, ranging from 683.54 to 5092.52 mg/L, with an average of 1853.15 mg/L. The Na^+ was the dominant cation in the groundwater in the northwest area, ranging from 100.30 to 533.10 mg/L, with an average of 269.59 mg/L, while the Cl^- was the dominant anion, ranging from 213.00 to 3788.00 mg/L, with an average of 1067.20 mg/L. Indeed, the Cl^- and Na^+ contents in the whole area were high, which is consistent with the Na-Cl hydrochemical type, indicating that this area was severely affected by seawater intrusion.

The pH values of groundwater in the eastern area ranged from 5.11 to 6.94, with an average of 6.30. In addition, the range of TDS was relatively small, ranging from 96.43 to 626.78 mg/L, with an average of 352.64 mg/L. The dominant cations in the groundwater were Na^+ and Ca^{2+}, with average values of 66.29 and 46.78 mg/L, respectively. On the other hand, the dominant anion was HCO_3^-, ranging from 69.78 to 265.15 mg/L, with an average of 154.65 mg/L. It can be seen from the Piper diagram that Na-HCO_3 and Ca-HCO_3 were the main hydrochemical facies in the eastern area, indicating that this area was the least affected by seawater intrusion.

In terms of the average ion concentrations, the three areas were not evenly distributed, reflecting the different

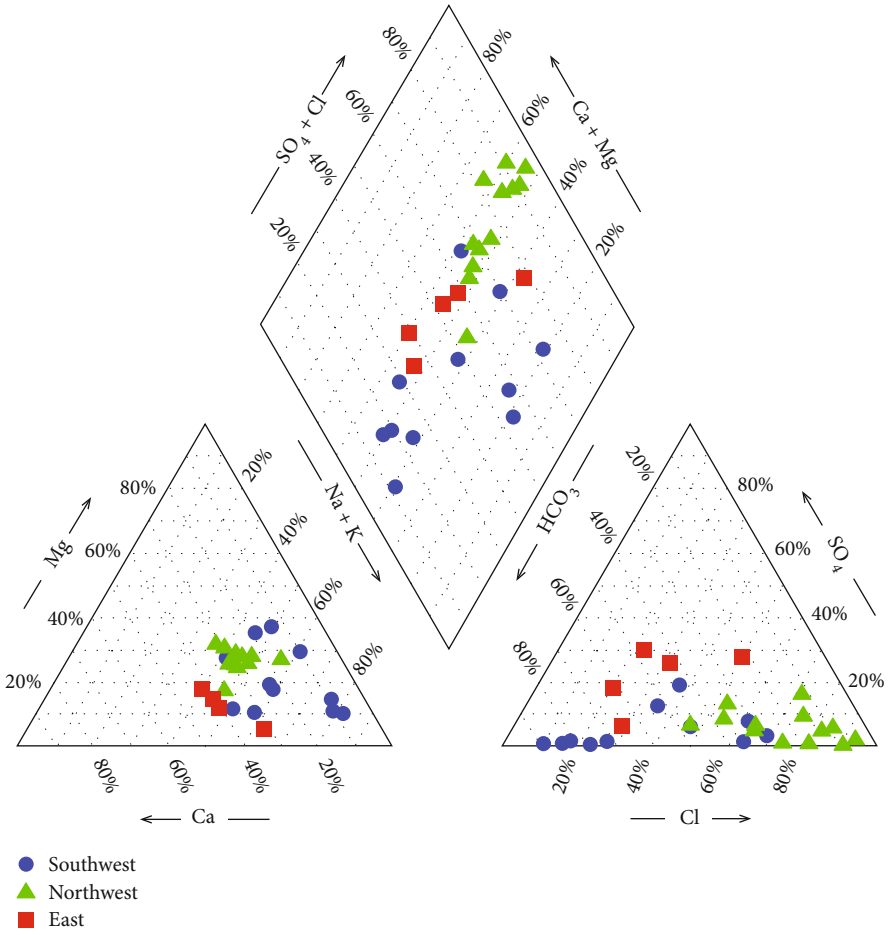

Figure 3: Piper diagram of the hydrochemical composition of groundwater.

spatial magnitude of the impact of seawater intrusion. The seawater intrusion in the western area was more serious, especially in the northwestern area, while that observed in the eastern area was relatively slight. The groundwater chemical type in the entire study area was first Ca(Mg)-HCO_3, then transformed into Na(Ca/Mg)-HCO_3 and Na(Ca/Mg)-Cl, and finally transformed into Na-Cl as a result of seawater intrusion.

3.1.2. Distribution of ^{222}Rn in Groundwater. The average of the field survey data showed a great spatial variation in the ^{222}Rn activity. Indeed, the spatial amplitude of variation was about 50 times (Figure 4). The ^{222}Rn activity ranged from 987.96 to 49858.91 Bq/m^3, with an average value of 15560.06 Bq/m^3. The average activity values of ^{222}Rn were 20417.67, 10525.17, and 17964.33 Bq/m^3 in the southwestern, northwestern, and eastern areas, respectively.

Generally, the activity of ^{222}Rn in groundwater is fundamentally determined by the type and abundance of uranium-bearing minerals in the parent rock. Various uranium-bearing minerals in the strata decay continuously to produce ^{222}Rn, resulting in the high activity of ^{222}Rn in groundwater, especially in confined aquifers. Influenced by geological background, the activity of ^{222}Rn in magmatic rocks is higher than that in sedimentary and metamorphic rocks [33]. The sampling sites in the southwestern and eastern areas are mainly located in the magmatic rock area. Therefore, the average activity of ^{222}Rn in these areas is higher than that of the northwestern area, which is characterized by the presence of Quaternary loose sediments. Compared with the distribution of ^{222}Rn isotope in the four watersheds around Jiaozhou Bay [34], the average activity of ^{222}Rn in the Dagu River Basin with loose Quaternary sediments was 4399 Bq/m^3, which is significantly lower than those in Licun River, Moshui-Baisha River, and Yang River. In the three other watersheds where the sampling sites are mostly located in the Mesozoic acidic magmatic rock area, the average activity of ^{222}Rn ranged from 13342 to 17234 Bq/m^3.

The contents of uranium and radium in magmatic rocks were relatively high. The parent of ^{222}Rn is ^{226}Ra, both of which belong to the ^{238}U series. The activity of ^{238}U can directly determine the activity of ^{222}Rn [34]. Indeed, the results revealed a positive correlation between ^{222}Rn and ^{238}U (Figure 5).

However, low ^{238}U and high ^{222}Rn values were observed in TW1, TW2, TW5, TE1, and TE5. Br^- is stable in nature and is mainly found in the ocean. Thus, Br^- can be used to identify the source of salt in coastal groundwater [35]. The Br/Cl ratios in these samples were quite different from

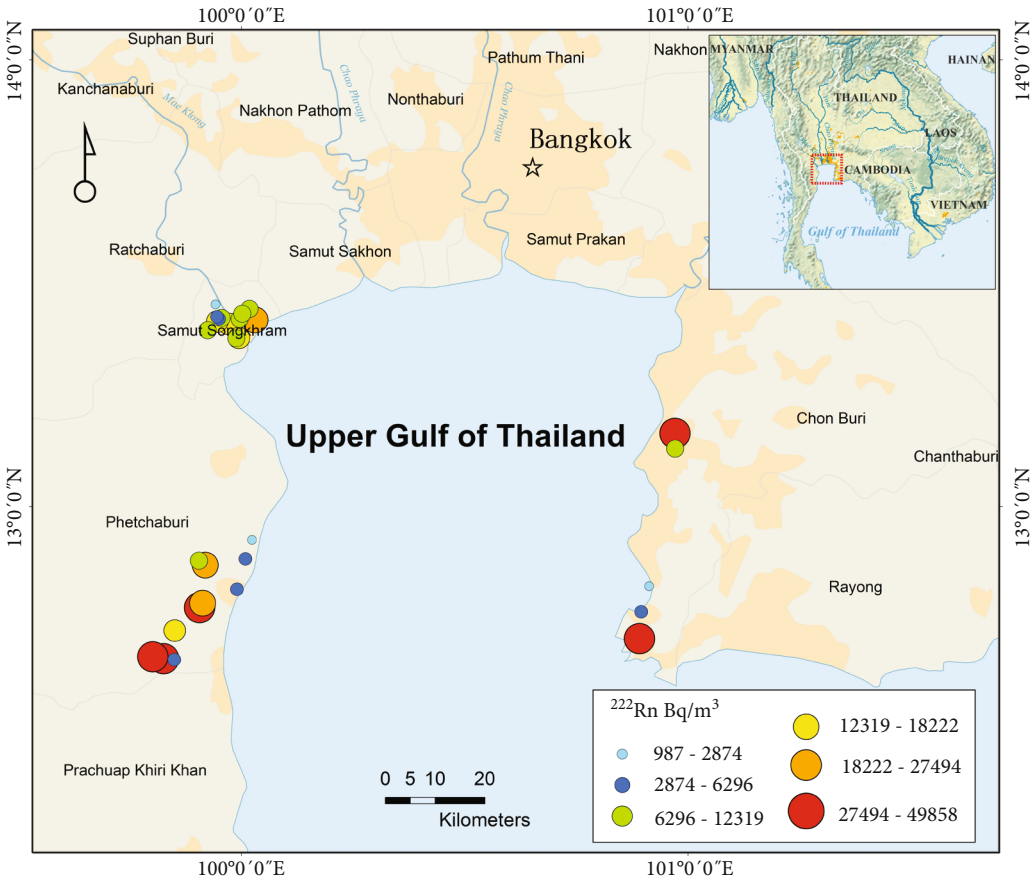

Figure 4: Distribution of ^{222}Rn in groundwater in the Upper Gulf of Thailand.

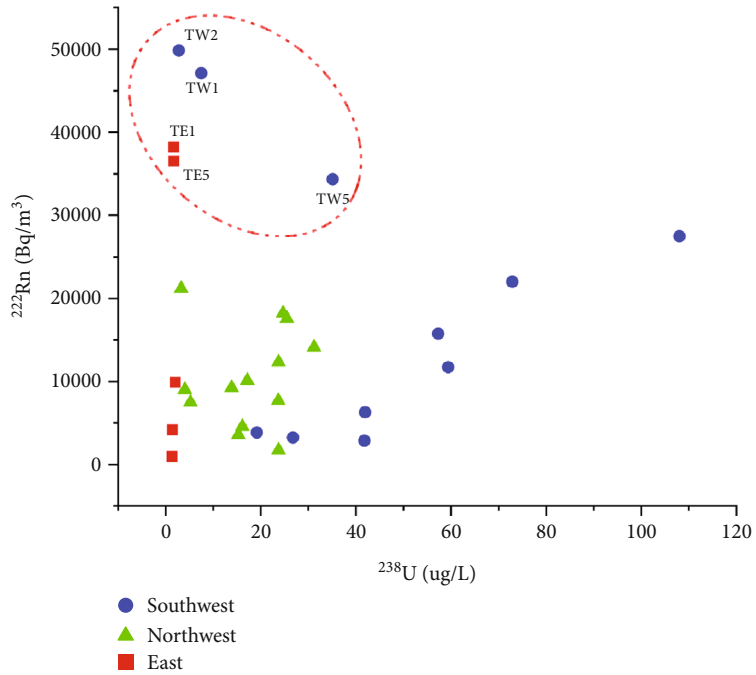

Figure 5: Correlation analysis between ^{238}U and ^{222}Rn.

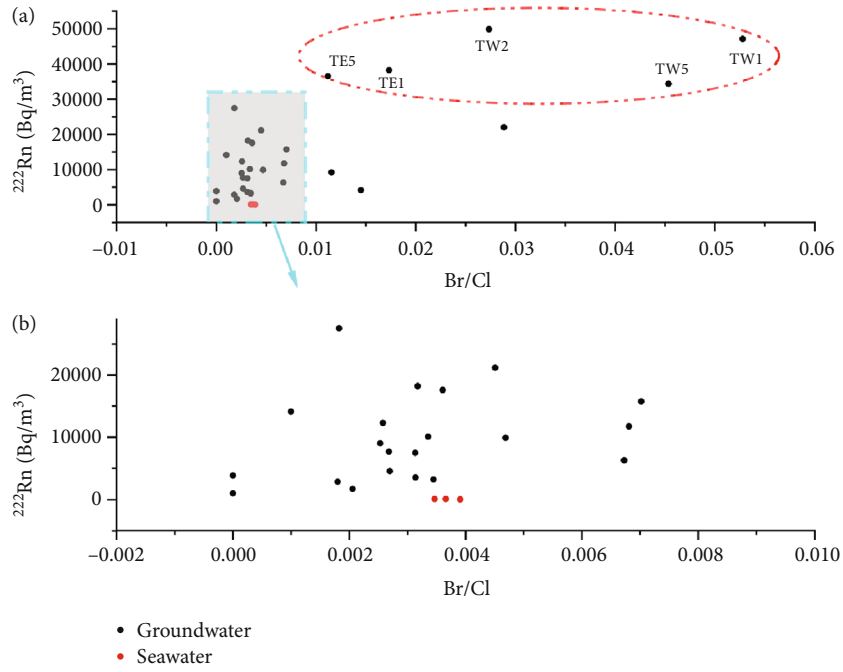

Figure 6: ^{222}Rn versus Br/Cl for groundwater and seawater (a) and samples with Br/Cl values between 0 and 0.008 were independently plotted (b).

seawater (Figure 6), suggesting that these groundwaters have little interaction with seawater. Therefore, the sampling site is relatively closed, with a long water residence time and a significant water-rock interaction, leading to high radon levels.

The results showed that the activity of ^{222}Rn in groundwater is mainly controlled by the geological background. Indeed, the geological background controls its activity mainly by the lithology of the aquifer. Moreover, other factors may affect the geochemical behavior of ^{222}Rn in groundwater, such as groundwater sources, contact with air, recharge conditions, rock fissures and soil voids, water retention time, and water-rock interaction time [33, 34].

3.2. SGD Flux Estimation. SGD is an important channel for transporting terrestrial materials to the ocean [1], and it is one of the main causes of nearshore hypoxia and acidification [18, 36]. SGD might have a role in the coastal pollution that has been reported to be a tool to reveal offshore pollution from the large industrial complex in the Gulf of Thailand [22].

The hydrochemical types of groundwater along the Gulf of Thailand, as well as the activity, distribution, and influencing factors of ^{222}Rn isotope, were first determined to better use ^{222}Rn as a tracer to study various oceanographic processes. A ^{222}Rn mass balance model was built to estimate the submarine groundwater discharge in the Upper Gulf of Thailand.

3.2.1. Estimation of SGD Fluxes in the East Coast of the Gulf of Thailand. The ^{222}Rn mass balance model proposed by Burnett and Dulaiova and Charette et al. was used to evaluate the SGD in the East coast of the Gulf of Thailand (Figure 7) and speculate the changes in SGD with tides [10, 37].

The radon inventory needs to be determined in seawater to estimate the total groundwater flux. Indeed, the ^{222}Rn flux from SGD can be calculated based on the main sources and losses of ^{222}Rn in the radon inventory (Equation (1)). This ^{222}Rn flux can be converted to groundwater flux by dividing the derived ^{222}Rn fluxes by the groundwater ^{222}Rn end-member, according to the following equation:

$$F_{\mathrm{SGD}} = I\lambda - F_{\mathrm{sed}} - F_{\mathrm{riv}} + F_{\mathrm{atm}} + F_{\mathrm{mix}}, \tag{1}$$

$$Q = \frac{F_{\mathrm{SGD}}}{A_{\mathrm{gw}}}. \tag{2}$$

where Q is the SGD fluxes (m/d); F_{SGD} denotes the ^{222}Rn flux input by SGD (Bq/(m^2·d)); I denotes the activity of ^{222}Rn in the radon inventory (Bq/m^2), which is equal to the depth of water multiplied by the radon activity at that depth; λ is the decay constant of ^{222}Rn (0.181 d^{-1}); F_{sed} denotes the sediment diffusion fluxes (Bq/(m^2·d)); F_{riv} is the river input fluxes (Bq/(m^2·d)); F_{atm} denotes the fluxes of ^{222}Rn from the sea surface to the atmosphere (Bq/(m^2·d)); F_{mix} denotes the mixed loss fluxes caused by mixing with low-activity seawater outside the bay (Bq/(m^2·d)); and A_{gw} denotes the ^{222}Rn activity in groundwater (Bq/m^3).

This paper refers to the data of the activity of ^{222}Rn in the radon inventory used by Burnett et al. [23] to estimate SGD in the East coast of the Gulf of Thailand in July 2018. The average value of the activity of ^{222}Rn in the radon inventory was 173.00 Bq/m^2.

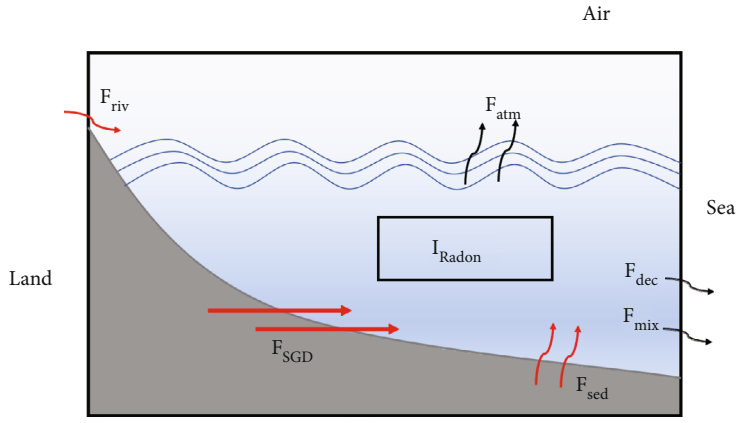

Figure 7: ^{222}Rn mass balance model (modified by Burnett and Dulaiova [10]).

^{222}Rn can spread from sediment to water when the activity of ^{222}Rn in the sediment pore water is greater than that of the overlying water. Martens et al. [38] proposed the following equation for calculating the sediment diffusion flux:

$$F_{sed} = (\lambda D_s)^{0.5}\left(C_{eq} - C_o\right), \tag{3}$$

where D_s is the effective sediment diffusion coefficient; C_{eq} is the activity of radon in the pore water, estimated to be 5900.00 Bq/m^3; and C_0 is the activity of radon in the overlying water estimated to be 73.10 Bq/m^3 [23]. When sediment porosity n ranges from 0.2 to 0.7, D_s can be approximately equal to the molecular diffusion coefficient (D_0) of ^{222}Rn of the sediment porosity n [39]. In this study, the sediment porosity n was set at 0.62 [23]. D_0 is related to temperature because the sediments spread on the seabed; thus, the T value was taken to be equal to 29°C at the bottom of seawater.

$$D_S = nD_0, \tag{4}$$

$$D_0 = 10^{-\left(\frac{980}{273.15+T}+1.59\right)}. \tag{5}$$

By considering the value of the bottom temperature in Equation (5), D_o is 1.48×10^{-5} cm^2/s (1.28×10^{-4} m^2/d). Therefore, D_s is equal to 7.94×10^{-5} m^2/d. F_{sed} is equal to 22.14 Bq/(m^2·d).

The contribution of rivers to SGD is very limited. Indeed, the rivers that flow into the bay are Mae Klong River, Tha Chin River, Chao Phraya River, and Bang Pakong River. The average flow of the four rivers recorded in November was 800 m/s [40], equivalent to 6.91×10^7 m/d. The activity of radon in rivers was very low, and the difference of the activity between all rivers was small. Field measurements of radon activity were made in two river water samples from the lower reaches of Mae Klong River. The radon activity of the two groups of river water samples is 158.03 and 224.65 Bq/m^3, respectively. So the average activity of ^{222}Rn in river water was 191.34 Bq/m^3. The area of the upper Gulf of Thailand is approximately 1×10^{10} m^2. The F_{riv} is, therefore, equal to 1.32 Bq/(m^2·d).

Similar to the water-rock interface, there is also an exchange of radon at the water-air interface. Macintyre et al. [41] proposed the equation for estimating the loss flux of atmospheric escape:

$$F_{atm} = k(C_w - \alpha C_a), \tag{6}$$

where k is the gas migration coefficient. Its value is mainly related to wind speed [42]. In this study, the wind speed value was considered to be 0.5 m/s. The K value is equal to 0.9 cm/h (0.216 m/d) when the wind speed value is less than 1.5 m/s [42]. In order to accurately measure the radon activity in surface water, two seawater samples near TES1 were also tested for radon activity in the field. The radon activity of TE1 is 108.86 Bq/m^3, and the radon activity of the other two seawater samples is 73.82 and 36.62 Bq/m^3, respectively. The activity of radon in C_w surface water was 73.10 Bq/m^3. C_a is the ^{222}Rn activity value in air. This value was considered to be equal to 0. α is the ratio of ^{222}Rn activity in water to ^{222}Rn activity in the atmosphere. This ratio depends on the temperature of the water vapor phase. Based on the above values, the F_{atm} is equal to 15.79 Bq/(m^2·d).

F_{mix} denotes the loss from mixing with low radon water from the open sea. When sediment diffusion, river input, and atmospheric escape loss fluxes were calculated, the ^{222}Rn activity in the radon inventory was only affected by SGD and mixed loss flux [18]. The maximum negative value of variation in radon inventory was chosen as the mixing loss [10, 41]. This method underestimates the mixed loss, since each period may have a specific mixed loss and SGD input and the mixing loss value should be larger to offset the radon flux carried by SGD. The underestimated estimate of mixing loss leads to the underestimated estimate of SGD according to Equation (1). [43]. The results showed a F_{mix} value of 282.00 Bq/(m^2·d).

Based on the flux values mentioned above and Equation (1), an F_{SGD} value of 305.64 Bq/(m^2·d) was obtained.

The activity of ^{222}Rn in groundwater at different times was determined using the continuous monitoring data of groundwater. The following results are the Q values obtained, considering the F_{SGD} value into the ^{222}Rn activity in different periods in Table 3.

Table 3: SGD fluxes in different time periods.

Sample code	^{222}Rn (Bq/m^3)	SGD fluxes (m/d)	Sample code	^{222}Rn (Bq/m^3)	SGD fluxes (m/d)
CM1	3712.51	0.0823	CM8	3659.13	0.0835
CM2	3767.10	0.0811	CM9	3448.26	0.0886
CM3	3533.41	0.0865	CM10	3122.24	0.0979
CM4	3486.32	0.0877	CM11	2949.66	0.1036
CM5	3180.83	0.0961	CM12	2785.26	0.1097
CM6	3241.52	0.0943	CM13	3088.22	0.0990
CM7	3470.15	0.0881	CM14	3327.69	0.0918

The average, maximum, and minimum groundwater flux values observed on the East coast of the Gulf of Thailand were 0.0922, 0.1097, and 0.0811 m/d, respectively. Although the F_{SGD} estimate is relatively conservative, the ^{222}Rn activity at the continuous monitoring sites was relatively low compared to that in the entire Gulf of Thailand coast. Thus, the average groundwater flux estimated for the East coast of the Gulf of Thailand was relatively high.

3.2.2. Impact of Tides on SGD. The tidal heights observed during the period from 6:00 on November 23, 2018, to 17:00 on November 24, 2018, are reported in Table 4. It can be seen that the first low tide height value (2.4 m) was observed at 12:00 on November 23, while the first high tide height value (2.7 m) was at 14:00-15:00. On the other hand, the second low tide height value (1.2 m) was observed at 22:00-23:00 on November 23, while the second high tide height value (3.1 m) was recorded at 7:00 the next day (Figure 8). The average tidal height value during this period was 2.43 m. The first and second tidal ranges were 0.3 and 1.9 m, respectively. In addition, the second tidal range was larger and the time span was longer.

Electrical resistivity tomography was used to monitor the influence range of tidal action (provided in Supporting-Information). The results (Fig. S1) showed that the formation resistivity near the continuous monitoring well changed with tides and the salt-freshwater interface moved constantly, which indicated that this site was affected by tidal action and the exchange of groundwater and seawater took place. Radon activity changed with tidal height. We compared tides with SGD, as the SGD was the result of changes in radon activity.

By comparing the SGD with the tidal data (Figure 8), we found that the groundwater flux and the tide were negatively correlated, and the response of the groundwater flux to the tidal height change showed a certain hysteresis. This may be due to the intrusion of seawater into the aquifer as a result of rising tides, which is not conducive to the discharge of submarine groundwater. However, when tides fall, groundwater can be discharged from the aquifer, which is conducive to submarine groundwater discharge.

At the first high tide, which was 2.9 m, the SGD was 0.0811 m/d; at the first low tide, which was 2.4 m, the SGD was 0.0961 m/d; at the second high tide, which was 2.7 m, the SGD was 0.0835 m/d; at the second low tide, which was 1.2 m, the SGD was 0.1097 m/d. The SGD observed during low tide was about 1.25 times higher than that observed during high tide.

Table 4: Results of the tidal height.

Time	Tidal height (m)	Time	Tidal height (m)
2018/11/23 6:00	2.9	2018/11/24 0:00	1.4
2018/11/23 7:00	2.9	2018/11/24 1:00	1.6
2018/11/23 8:00	2.8	2018/11/24 2:00	1.9
2018/11/23 9:00	2.6	2018/11/24 3:00	2.3
2018/11/23 10:00	2.6	2018/11/24 4:00	2.6
2018/11/23 11:00	2.5	2018/11/24 6:00	3.0
2018/11/23 12:00	2.4	2018/11/24 7:00	3.1
2018/11/23 13:00	2.6	2018/11/24 8:00	3.0
2018/11/23 14:00	2.7	2018/11/24 9:00	2.9
2018/11/23 15:00	2.7	2018/11/24 10:00	2.8
2018/11/23 16:00	2.6	2018/11/24 11:00	2.7
2018/11/23 17:00	2.5	2018/11/24 12:00	2.7
2018/11/23 18:00	2.2	2018/11/24 13:00	2.7
2018/11/23 19:00	1.9	2018/11/24 14:00	2.7
2018/11/23 20:00	1.6	2018/11/24 15:00	2.7
2018/11/23 21:00	1.4	2018/11/24 16:00	2.7
2018/11/23 22:00	1.2	2018/11/24 17:00	2.5
2018/11/23 23:00	1.2		

3.2.3. Estimation of SGD Fluxes on the Gulf of Thailand. The F_{SGD} was estimated to assess the groundwater discharge fluxes across the Gulf of Thailand from the East coast of the Gulf of Thailand to the entire Gulf of Thailand. The average activity values of ^{222}Rn observed in the southwestern, northwestern, and eastern areas were 20417.67, 10525.17, and 17964.33 Bq/m^3, respectively. Therefore, based on Equation (2), the estimated groundwater discharge flux values in the southwestern, northwestern, and eastern areas were 0.0150, 0.0290, and 0.0170 m/d, respectively, while the average groundwater discharge flux of the entire Gulf of Thailand was 0.0203 m/d.

Few studies on the SGD fluxes in the Gulf of Thailand were carried out. The results of the current study were compared with results obtained in the Gulf of Thailand and other regions worldwide. The results are reported in Table 5. The results of the current study were in line with

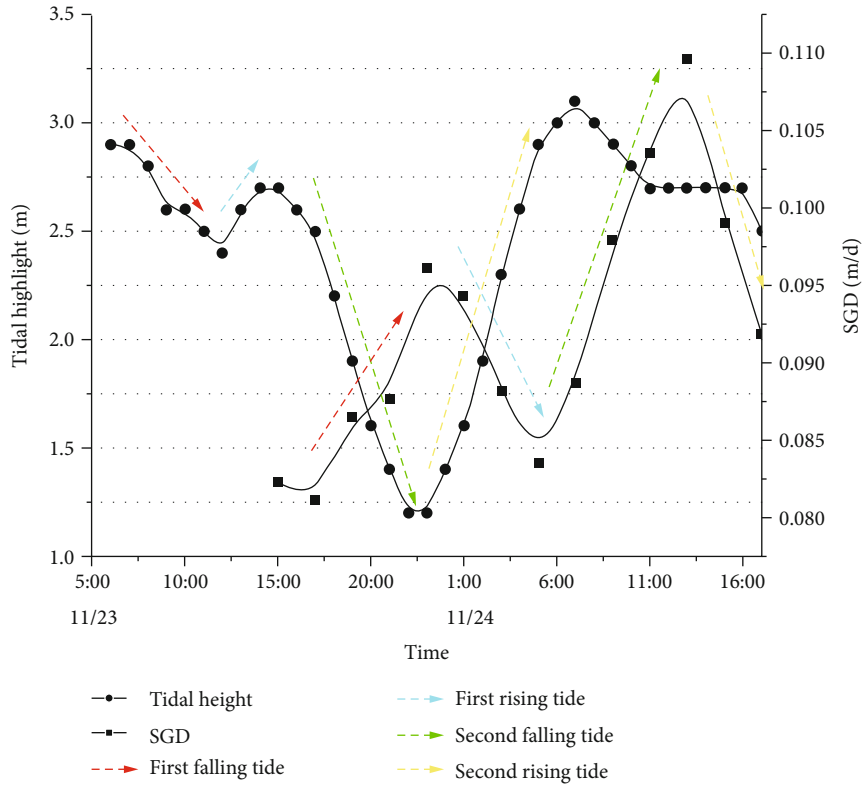

Figure 8: Relationship between tides and SGD fluxes on the East coast of the Gulf of Thailand, 23-24 November 2018.

Table 5: Comparison of SGD fluxes in the Gulf of Thailand and other regions.

Research region	Date	SGD (m/d)	Approach	Reference
East coast of the Gulf of Thailand	2004	0.019	Seepage meters	Burnett et al. [28]
East coast of the Gulf of Thailand	2017	0.04-0.14	^{222}Rn	Burnett et al. [23]
East coast of the Gulf of Thailand	2018	0.0922	^{222}Rn	This study
Gulf of Thailand	2018	0.0203	^{222}Rn	This study
Sarasota Bay, USA	2002-2006	0.007-0.24	Seepage meters, ^{222}Rn and CH_4	Mwashote et al. [44]
Ubatuba, Brazil	2003	0.01-0.29	^{222}Rn	Burnett et al. [45]
Laizhou Bay, China	2012	0.089-0.103	^{224}Ra	Wang et al. [2]
Laizhou Bay, China	2014	0.102-0.15	^{224}Ra,^{224}Ra,^{226}Ra and ^{222}Rn	Zhang et al. [46]
Yellow River Estuary, China	2014	0.09-1.06	^{224}Ra and ^{226}Ra	Chen et al. [36]

those reported by other authors. However, the difference in the results of the current study may be due to the ignorance of some parameters with little influence in the model used and the estimation of some parameters. Furthermore, the difference in time scale and space scale, as well as measurement errors, may also affect the final results.

4. Conclusions

The activity of radon isotope in groundwater along the Gulf of Thailand showed a great spatiotemporal variation, but it was not affected by seawater intrusion. The relationship between radon isotope and Br/Cl ratio suggested an impact of the residence time and salinization mechanism of groundwater on the change in radon activity. The correlation between radon isotope and ^{238}U suggested that the distribution of radon isotope in the aquifer is controlled by the geological environment, especially the content of ^{226}Ra (which is the parent of ^{222}Rn).

The F_{SGD} value of the East coast of the Gulf of Thailand was 305.64 Bq/(m^2·d). Based on the radon activity in groundwater, the average submarine groundwater flux on the East coast of the top of the Gulf of Thailand was estimated to be 0.0922 m/d, while that on the submarine groundwater flux of the entire Gulf of Thailand was 0.0203 m/d. The tide was the main factor affecting the

submarine groundwater discharge. The results showed that the SGD on the East coast of the Gulf of Thailand was negatively correlated with the tidal height. The SGD observed during low tide was about 1.25 times higher than that observed during high tide.

Data Availability

The data are listed in the Supplementary Materials.

Conflicts of Interest

The authors declare that they have no conflicts of interest.

Acknowledgments

We thank staff from Marine and Coastal Resources Research and Development Institute and Phuket Marine Biological Center. This work was supported by the National Natural Science Foundation of China-Shandong Joint Fund for Marine Science Research Centers (Nos. U2106203, U1806212), National Natural Science Foundation of China (41706067), and China-Thailand Cooperation Project "Research on Vulnerability of Coastal Zones."

Supplementary Materials

The supplementary file includes Table S1 and Fig. S1. Table S1: the original data collected from the 2018 in the Upper Gulf of Thailand which presents the electrical conductivity and radon activity of groundwater samples at the continuous monitoring sites. Fig. S1: the result of the electrical resistivity tomography. The E60 instrument produced by GEOPEN (BJ, China) was used. Data acquisition was carried out using Wenner electrode configurations. The starting point is 100.90° E, 12.77° N, and the end point is 100.90° E, 12.77° N. A total of 80 stainless steel electrodes (spaced 2 m apart) were used and covered a total length of 200 m. Fig. S1 shows that the salt-freshwater interface (30 Ω·m) in the region has been altered by tidal action. *(Supplementary Materials)*

References

[1] W. C. Burnett, H. Bokuniewicz, M. Huettel, W. S. Moore, and M. Taniguchi, "Groundwater and pore water inputs to the coastal zone," *Biogeochemistry*, vol. 66, no. 1-2, pp. 3–33, 2003.

[2] X. Wang, H. Li, J. J. Jiao et al., "Submarine fresh groundwater discharge into Laizhou Bay comparable to the Yellow River flux," *Scientific Reports*, vol. 5, no. 1, 2015.

[3] G. Kim, J. W. Ryu, H. S. Yang, and S. T. Yun, "Submarine groundwater discharge (SGD) into the Yellow Sea revealed by ^{228}Ra and ^{226}Ra isotopes: implications for global silicate fluxes," *Earth and Planetary Science Letters*, vol. 237, no. 1-2, pp. 156–166, 2005.

[4] P. W. Swarzenski, C. Reich, K. D. Kroeger, and M. Baskaran, "Ra and Rn isotopes as natural tracers of submarine groundwater discharge in Tampa Bay, Florida," *Marine Chemistry*, vol. 104, no. 1-2, pp. 69–84, 2007.

[5] M. A. Charette, M. E. Gonneea, P. J. Morris et al., "Radium isotopes as tracers of iron sources fueling a Southern Ocean phytoplankton bloom," *Deep Sea Research Part II: Topical Studies in Oceanography*, vol. 54, no. 18-20, pp. 1989–1998, 2007.

[6] G. Wang, W. Jing, S. Wang et al., "Coastal acidification induced by tidal-driven submarine groundwater discharge in a coastal coral reef system," *Environmental Science & Technology*, vol. 48, no. 22, pp. 13069–13075, 2014.

[7] V. Rodellas, J. Garcia-Orellana, P. Masqué, M. Feldman, and Y. Weinstein, "Submarine groundwater discharge as a major source of nutrients to the Mediterranean Sea," *Proceedings of the National Academy of Sciences of the United States of America*, vol. 112, no. 13, pp. 3926–3930, 2015.

[8] I. R. Santos, X. Chen, A. L. Lecher et al., "Submarine groundwater discharge impacts on coastal nutrient biogeochemistry," *Nature Reviews Earth & Environment*, vol. 2, no. 5, pp. 307–323, 2021.

[9] W. S. Moore, "Large groundwater inputs to coastal waters revealed by ^{226}Ra enrichments," *Nature*, vol. 380, no. 6575, pp. 612–614, 1996.

[10] W. C. Burnett and H. Dulaiova, "Estimating the dynamics of groundwater input into the coastal zone via continuous radon-222 measurements," *Journal of Environmental Radioactivity*, vol. 69, no. 1-2, pp. 21–35, 2003.

[11] V. Rodellas, J. Garcia-Orellana, G. Trezzi et al., "Using the radium quartet to quantify submarine groundwater discharge and porewater exchange," *Geochimica et Cosmochimica Acta*, vol. 196, pp. 58–73, 2017.

[12] J. Gao, X. Wang, Y. Zhang, and H. L. Li, "Estimating submarine groundwater discharge and associated nutrient inputs into Daya Bay during spring using radium isotopes," *Water Science and Engineering*, vol. 11, no. 2, pp. 120–130, 2018.

[13] X. Wang, H. Li, Y. Zhang, W. Qu, and M. Schubert, "Submarine groundwater discharge revealed by ^{222}Rn: comparison of two continuous on-site ^{222}Rn-in-water measurement methods," *Hydrogeology Journal*, vol. 27, no. 5, pp. 1879–1887, 2019.

[14] S. Lamontagne and I. T. Webster, "Cross-shelf transport of submarine groundwater discharge tracers: a sensitivity analysis," *Journal of Geophysical Research: Oceans*, vol. 124, no. 1, pp. 453–469, 2019.

[15] S. Lamontagne and I. T. Webster, "Theoretical assessment of the effect of vertical dispersivity on coastal seawater radium distribution," *Frontiers in Marine Science*, vol. 6, p. 357, 2019.

[16] Y. Zhang, H. Li, X. Wang et al., "Estimation of submarine groundwater discharge and associated nutrient fluxes in eastern Laizhou Bay, China using ^{222}Rn," *Journal of Hydrology*, vol. 533, pp. 103–113, 2016.

[17] E. Petermann, K. Knöller, C. Rocha et al., "Coupling end-member mixing analysis and isotope mass balancing (222-Rn) for differentiation of fresh and recirculated submarine groundwater discharge into Knysna Estuary, South Africa," *Journal of Geophysical Research: Oceans*, vol. 123, no. 2, pp. 952–970, 2018.

[18] X. Guo, B. Xu, W. C. Burnett et al., "Does submarine groundwater discharge contribute to summer hypoxia in the Changjiang (Yangtze) River Estuary?," *Science of the Total Environment*, vol. 719, article 137450, 2020.

[19] P. Muthukumar, S. Selvam, D. S. S. Babu et al., "Measurement of submarine groundwater discharge (SGD) into Tiruchendur coast at southeast India using ^{222}Rn as a naturally occurring tracer," *Marine Pollution Bulletin*, vol. 174, article 113233, 2022.

[20] M. Cerdà-Domènech, V. Rodellas, A. Folch, and J. Garcia-Orellana, "Constraining the temporal variations of Ra isotopes and Rn in the groundwater end-member: implications for derived SGD estimates," *Science of the Total Environment*, vol. 595, pp. 849–857, 2017.

[21] G. Wattayakorn, "Environmental Issues in the Gulf of Thailand," in *The Environment in Asia Pacific Harbours*, E. Wolanski, Ed., pp. 249–259, Springer, Dordrecht, 2006.

[22] H. Dulaiova and W. C. Burnett, "Radon loss across the water-air interface (Gulf of Thailand) estimated experimentally from ^{222}Rn-^{224}Ra," *Geophysical Research Letters*, vol. 33, no. 5, 2006.

[23] W. C. Burnett, P. Sola, S. Chanyotha, B. Bidorn, R. Kritsananuwat, and N. Chinfak, "Tracing underground sources of pollution to coastal waters off Map Ta Phut, Rayong, Thailand," *Marine Pollution Bulletin*, vol. 148, pp. 75–84, 2019.

[24] X. Wang, H. Li, Y. Zhang, C. Zheng, and M. Gao, "Investigation of submarine groundwater discharge and associated nutrient inputs into Laizhou Bay (China) using radium quartet," *Marine Pollution Bulletin*, vol. 157, article 111359, 2020.

[25] N. Phien-wej, P. H. Giao, and P. Nutalaya, "Land subsidence in Bangkok, Thailand," *Engineering Geology*, vol. 82, no. 4, pp. 187–201, 2006.

[26] G. Y. Xiong, G. Q. Chen, X. Y. Xu et al., "A comparative study on hydrochemical evolution and quality of groundwater in coastal areas of Thailand and Bangladesh," *Journal of Asian Earth Sciences*, vol. 195, article 104336, 2020.

[27] D. S. Vinson, T. Tagma, L. Bouchaou, G. S. Dwyer, N. R. Warner, and A. Vengosh, "Occurrence and mobilization of radium in fresh to saline coastal groundwater inferred from geochemical and isotopic tracers (Sr, S, O, H, Ra, Rn)," *Applied Geochemistry*, vol. 38, pp. 161–175, 2013.

[28] W. C. Burnett, G. Wattayakorn, M. Taniguchi et al., "Groundwater-derived nutrient inputs to the Upper Gulf of Thailand," *Continental Shelf Research*, vol. 27, no. 2, pp. 176–190, 2007.

[29] J. Fornés and K. Pirarai, "Groundwater in Thailand," *Journal of Environmental Science & Engineering*, vol. 3, pp. 304–315, 2014.

[30] R. Bhattacharyya, J. Jana, B. Nath, S. J. Sahu, D. Chatterjee, and G. Jacks, "Groundwater As mobilization in the Bengal Delta Plain, the use of ferralite as a possible remedial measure–a case study," *Applied Geochemistry*, vol. 18, no. 9, pp. 1435–1451, 2003.

[31] B. Nath, J. P. Maity, J. S. Jean et al., "Geochemical characterization of arsenic-affected alluvial aquifers of the Bengal Delta (West Bengal and Bangladesh) and Chianan Plains (SW Taiwan): implications for human health," *Applied Geochemistry*, vol. 26, no. 5, pp. 705–713, 2011.

[32] W. C. Burnett, G. Kim, and D. Lane-Smith, "A continuous radon monitor for assessment of radon in coastal ocean waters," *Journal of Radioanalytical and Nuclear Chemistry*, vol. 249, no. 1, pp. 167–172, 2001.

[33] W. Zhuo, T. Iida, and X. Yang, "Occurrence of ^{222}Rn, ^{226}Ra, ^{228}Ra and U in groundwater in Fujian Province, China," *Journal of Environmental Radioactivity*, vol. 53, no. 1, pp. 111–120, 2001.

[34] F. Pan, Z. Guo, Z. Ma, B. Zhang, and X. Yuan, "Distribution characteristics and influence factors of ^{222}Rn in riverine water and groundwater around Jiaozhou Bay," *Journal of Nuclear and Radiochemistry*, vol. 37, no. 6, pp. 490–496, 2015.

[35] G. Xiong, Q. An, T. Fu, G. Chen, and X. Xu, "Evolution analysis and environmental management of intruded aquifers of the Dagu River Basin of China," *Science of the Total Environment*, vol. 719, article 137260, 2020.

[36] G. Chen, B. Xu, S. Zhao et al., "Submarine groundwater discharge and benthic biogeochemical zonation in the Huanghe River Estuary," *Acta Oceanologica Sinica*, vol. 41, no. 1, pp. 11–20, 2022.

[37] M. A. Charette, W. S. Moore, and W. C. Burnett, "Chapter 5 uranium- and thorium-series nuclides as tracers of submarine groundwater discharge," *Radioactivity in the Environment*, vol. 13, pp. 155–191, 2008.

[38] C. S. Martens, G. W. Kipphut, and J. V. Klump, "Sediment-water chemical exchange in the coastal zone traced by in situ radon-222 flux measurements," *Science*, vol. 208, no. 4441, pp. 285–288, 1980.

[39] W. J. Ullman and R. C. Aller, "Diffusion coefficients in nearshore marine sediments1," *Limnology and Oceanography*, vol. 27, no. 3, pp. 552–556, 1982.

[40] A. Buranapratheprat, T. Yanagi, and S. Matsumura, "Seasonal variation in water column conditions in the upper Gulf of Thailand," *Continental Shelf Research*, vol. 28, no. 17, pp. 2509–2522, 2008.

[41] S. MacIntyre, R. Wanninkof, and J. P. Chanton, "Trace gas exchange across the air-water interface in freshwater and coastal marine environments," in *Biogenic Trace Gases: Measuring Emissions from Soil and Water. Methods in Ecology*, P. A. Matson and R. C. Harriss, Eds., pp. 52–97, Blackwell Science, Ltd., Cambridge, Mass, 1995.

[42] M. J. Lambert and W. C. Burnett, "Submarine groundwater discharge estimates at a Florida coastal site based on continuous radon measurements," *Biogeochemistry*, vol. 66, no. 1-2, pp. 55–73, 2003.

[43] K. C. Tse and J. J. Jiao, "Estimation of submarine groundwater discharge in Plover Cove, Tolo Harbour, Hong Kong by ^{222}Rn," *Marine Chemistry*, vol. 111, no. 3-4, pp. 160–170, 2008.

[44] B. M. Mwashote, M. Murray, W. C. Burnett, J. Chanton, S. Kruse, and A. Forde, "Submarine groundwater discharge in the Sarasota Bay system: its assessment and implications for the nearshore coastal environment," *Continental Shelf Research*, vol. 53, pp. 63–76, 2013.

[45] W. C. Burnett, R. Peterson, W. S. Moore, and J. de Oliveira, "Radon and radium isotopes as tracers of submarine groundwater discharge - results from the Ubatuba, Brazil SGD assessment intercomparison," *Estuarine, Coastal and Shelf Science*, vol. 76, no. 3, pp. 501–511, 2008.

[46] Y. Zhang, H. Li, X. Wang, C. Wang, K. Xiao, and W. Qu, "Submarine groundwater discharge and chemical behavior of tracers in Laizhou Bay, China," *Journal of Environmental Radioactivity*, vol. 189, pp. 182–190, 2018.